

# PCCP

Accepted Manuscript



This is an *Accepted Manuscript*, which has been through the Royal Society of Chemistry peer review process and has been accepted for publication.

*Accepted Manuscripts* are published online shortly after acceptance, before technical editing, formatting and proof reading. Using this free service, authors can make their results available to the community, in citable form, before we publish the edited article. We will replace this *Accepted Manuscript* with the edited and formatted *Advance Article* as soon as it is available.

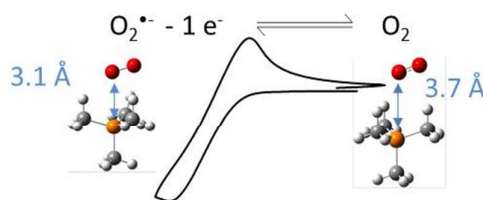
You can find more information about *Accepted Manuscripts* in the [Information for Authors](#).

Please note that technical editing may introduce minor changes to the text and/or graphics, which may alter content. The journal's standard [Terms & Conditions](#) and the [Ethical guidelines](#) still apply. In no event shall the Royal Society of Chemistry be held responsible for any errors or omissions in this *Accepted Manuscript* or any consequences arising from the use of any information it contains.

## Graphical abstract

# Insights into the reversible oxygen reduction reaction in a series of phosphonium-based ionic liquids

*Cristina Pozo-Gonzalo*<sup>\*a</sup>, *Patrick C. Howlett*<sup>a</sup>, *Jennifer L. Hodgson*<sup>b</sup>, *Louis A. Madsen*<sup>c</sup>,  
*Douglas R. MacFarlane*<sup>b</sup>, *Maria Forsyth*<sup>a</sup>



Extensive evidence for the stability of the superoxide anion in phosphonium-based ILs is demonstrated by computational quantum chemistry and NMR.

## Insights into the reversible oxygen reduction reaction in a series of phosphonium-based ionic liquids

Cite this: DOI: 10.1039/x0xx00000x

Cristina Pozo-Gonzalo<sup>\*a</sup>, Patrick C. Howlett<sup>a</sup>, Jennifer L. Hodgson,<sup>b</sup> Louis A. Madsen<sup>c</sup>, Douglas R. MacFarlane<sup>b</sup>, Maria Forsyth<sup>a</sup>

Received 00th January 2012,  
Accepted 00th January 2012

DOI: 10.1039/x0xx00000x

www.rsc.org/

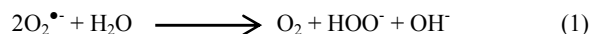
New findings supporting the stability of the superoxide ion,  $O_2^{\bullet-}$ , in the presence of the phosphonium cation,  $[P_{6,6,6,14}]^+$ , are presented. Extended electrochemical investigations of a series of neat phosphonium-based ILs with different anions, including chloride, bis(trifluoromethylsulfonyl)imide and dicyanamide, demonstrate the chemical reversibility of the oxygen reduction process. Quantum chemistry calculations show a short intermolecular distance ( $r = 3.128 \text{ \AA}$ ) between the superoxide ion and the phosphonium cation. NMR experiments have been performed to assess the degree of long term degradation of  $[P_{6,6,6,14}]^+$ , in the presence of superoxide and peroxide species, showing no chemically distinct degradation products of importance in reversible air cathodes.

### 1. Introduction

Energy storage devices with high energy and power density are required to support the advancement of a wide range of significant applications including electric vehicles, portable electronics and implantable devices. The search for alternative energy storage devices has been triggered by fluctuating prices and, more importantly, the long term sustainability of fossil fuels. At the moment the best available energy storage devices are based on Lithium-ion technologies because of their high energy density ( $200\text{--}250 \text{ Wh.kg}^{-1}$ ); these devices dominate the market for portable devices, power tools and more recently, small electric vehicles. Unfortunately, this technology has reached its theoretical limit<sup>2</sup> and cannot meet the needs of emerging applications because of insufficient energy density which is limited by the intercalation of ions into the electrode.<sup>3</sup>

On the other hand, metal-air batteries have emerged as potential, next-generation of energy storage devices because of their intrinsically high energy density values. As an example, the theoretical specific energy density of the Li-air system is close to  $5300 \text{ Wh.kg}^{-1}$ <sup>4</sup> and for Mg-air is close to  $2800 \text{ Wh.kg}^{-1}$ .<sup>5</sup> The key feature of this technology is the fact that the cathode reactant, oxygen, is not stored inside the battery and most of the battery volume is occupied by the anode. More importantly, the active material in the cathode is continuously and infinitely available. Other metal air-systems that are under active development include Al-air and Mg-air. However, there are still many technical challenges to be overcome before commercialization of this technology is likely, as discussed further below.

From the cathode point of view one of the major drawbacks arises from the reactivity of the species that are electro-generated from oxygen in the conventional aprotic solvents that are used as electrolyte media. Notably, the superoxide anion,  $O_2^{\bullet-}$ , has been described as unstable in the presence of water and protic additives, through an irreversible disproportionation reaction (equation 1),<sup>6,7</sup> which reduces the reversibility of this reaction in a rechargeable battery.<sup>8</sup>



Ionic liquids (ILs) are a promising class of electrolytes that can support the electrochemical generation of a stable superoxide ion<sup>9</sup> and, depending on the cation–anion combination, can offer many advantages such as low flammability, ionic conductivity, negligible vapour pressure and a wide electrochemical window. As a result, ionic liquids have been successfully applied in a number of energy-related applications, where they offer the possibility of designing ideal electrolytes for batteries, super-capacitors, actuators, dye sensitized solar cells and thermo-electrochemical cells.<sup>10</sup>

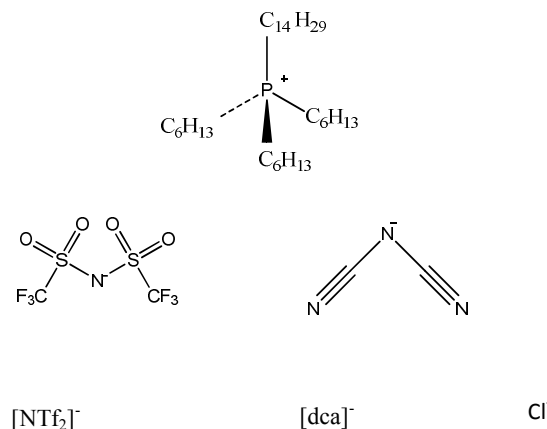
In order to explore new pathways toward rechargeable metal-air batteries, recent reports in the literature have described the chemical and/or electrochemical reversibility of the  $O_2/O_2^{\bullet-}$  redox couple in dry ionic liquids. In the literature, imidazolium, aliphatic and alicyclic ammonium based ionic liquids have been studied as media for the oxygen reduction reaction. It is now known that the superoxide anion is more stable in the aliphatic and alicyclic cation based ion liquids than in the imidazolium ILs, probably due to the

more localized charge in the former cases.<sup>11, 12</sup> In the imidazolium cation partial positive charges located on the 2, 4 and 5 positions of the ring render these prone to attack by nucleophilic agents. The role of protic additives has also been studied in ILs and has normally been found to be detrimental to the stability of the superoxide anion under such conditions.<sup>9, 13, 14</sup> In fact, the first published work on the oxygen reduction reaction investigated 1-ethyl-3-methylimidazolium chloride, [C<sub>2</sub>mim]Cl, mixed with aluminium chloride and showed that the electrogenerated superoxide species was unstable, with no reverse current being observed in cyclic voltammetry after the reduction of oxygen at scan rates of 5-200 mV s<sup>-1</sup>.<sup>15</sup> However, AlNashef *et al.*<sup>16</sup> reported evidence of the electrochemical generation of stable superoxide ions in 1-*n*-butyl-3-methylimidazolium hexafluorophosphate ([C<sub>4</sub>mim][PF<sub>6</sub>]), which was corroborated by Zhang *et al.*<sup>9</sup> in a series of 1-*n*-alkyl-3-methylimidazolium tetrafluoroborate ILs. The discrepancy among these findings in relation to the stability of superoxide was attributed to the presence of protic impurities in the [C<sub>2</sub>mim]AlCl<sub>4</sub> melt,<sup>15</sup> which exemplifies the detrimental role of protic additives to reversible O<sub>2</sub>/O<sub>2</sub><sup>•-</sup> redox couple.

More recently, the chemical reversibility of the O<sub>2</sub>/O<sub>2</sub><sup>•-</sup> redox couple, expressed in terms of the ratio of the anodic to cathodic current densities, ( $j_p^a / j_p^c$ ), was determined by Katayama *et al.*<sup>11</sup> in imidazolium and quaternary ammonium-based bis((trifluoromethyl)sulfonyl)imide, [NTf<sub>2</sub>], ionic liquids. They concluded that the superoxide ion was more stable in the presence of the aliphatic and alicyclic organic cations trimethyl-*n*-hexylammonium ([N<sub>622</sub><sup>+</sup>]), and 1-butyl-1-methylpyrrolidinium ([C<sub>4</sub>mpyr<sup>+</sup>]) ( $j_p^a / j_p^c$ : 0.97 and 0.93, respectively), but reacted with the aromatic cations 1-ethyl-3-methylimidazolium ([C<sub>2</sub>mim<sup>+</sup>]) and 1,2-dimethyl-3-propylimidazolium ([C<sub>3</sub>dmim<sup>+</sup>]) ( $j_p^a / j_p^c$ : 0.48 and 0.37, respectively). Other research groups have investigated the reversibility of the O<sub>2</sub>/O<sub>2</sub><sup>•-</sup> redox couple in dry ILs based on the trihexyl(tetradecyl)phosphonium cation, [P<sub>6,6,6,14</sub>]<sup>+</sup>, with both trifluorotris(pentafluoroethyl)phosphate, [FAP]<sup>-</sup> and bis((trifluoromethyl)sulfonyl)imide, [NTf<sub>2</sub>]<sup>-</sup>, anions and concluded that they cannot stabilise the superoxide anion O<sub>2</sub><sup>•-</sup>, and that therefore an irreversible reduction process is obtained.<sup>17, 18</sup> To explain this behaviour, Evans *et al.*<sup>18</sup> proposed a mechanism involving abstraction of the  $\alpha$ -proton from [P<sub>6,6,6,14</sub>]<sup>+</sup> by the superoxide ion to give a phosphorus ylide with a general structure R<sub>3</sub>P=CHR<sup>•</sup>.

On the contrary, the generation of a stable superoxide has been reported by Hayyan *et al.*<sup>19</sup> in [P<sub>6,6,6,14</sub>][NTf<sub>2</sub>]. More recently, we also reported the stability of superoxide anion in [P<sub>6,6,6,14</sub>]Cl<sup>20</sup> by cyclic voltammetry. As previously mentioned, protic additives, or impurities such as water, even at relatively low levels, reportedly can prevent the generation of stable superoxide in ILs.<sup>9</sup> However, our group has observed and reported the chemically reversible O<sub>2</sub>/O<sub>2</sub><sup>•-</sup> redox couple in [P<sub>6,6,6,14</sub>]Cl, not only under dry conditions, but also in the presence of large quantities of weak protic additives such as water (e.g. 1.5 and 4.5 wt % water).<sup>20</sup> We attributed the stabilising of the electrogenerated O<sub>2</sub><sup>•-</sup> in this phosphonium-based IL electrolyte to an ion-pairing interaction.<sup>20, 21</sup> Given these discrepancies in the reported results for neat phosphonium-based ILs and the observed stability of the superoxide in the [P<sub>6,6,6,14</sub>]Cl in the presence of protic additives, the aim of the present research work is to further investigate the interaction of the superoxide anion with the phosphonium cation using computational quantum chemistry and NMR. Furthermore, we have also extended the electrochemical investigation of the chemical reversibility of the oxygen reduction process to include a range of [P<sub>6,6,6,14</sub>]<sup>+</sup> based ILs with different anions, including chlorine, bis((trifluoromethyl)sulfonyl)imide and

dicyanamide (Scheme 1). These anions were selected based on different factors including size, acid/base character, hydrophobic/hydrophilic properties, and previously good performance as electrolytes for metal-air batteries (e.g. magnesium, zinc and lithium).<sup>22-24</sup>



**Scheme 1.** Ionic liquid cation and anions used in this work

## 2. Experimental

Trihexyl(tetradecyl)phosphonium chloride, [P<sub>6,6,6,14</sub>]Cl, (98%, Cytec), trihexyl(tetradecyl)phosphonium bis((trifluoromethyl)sulfonyl)imide, [P<sub>6,6,6,14</sub>][NTf<sub>2</sub>], (98%, iolitec) and trihexyl(tetradecyl)phosphonium dicyanamide, [P<sub>6,6,6,14</sub>][dca], (98%, Cytec) were purified by dissolving them in diethyl ether and washing with a 10% NaOH solution in a separating funnel. Then the organic phase was washed a few times with water until the pH of the water phase reached 7. Anhydrous sodium sulfate was added to the organic phase to remove any water present. After filtration, the organic phase was evaporated with a rotary evaporator, followed by a high vacuum pump system for two days to ensure low level of water content. The water contents were evaluated by Karl-Fischer titration and were 150 ppm for [P<sub>6,6,6,14</sub>]Cl, 200 ppm for [P<sub>6,6,6,14</sub>][NTf<sub>2</sub>], and 300 ppm for [P<sub>6,6,6,14</sub>][dca]. KO<sub>2</sub> and Na<sub>2</sub>O<sub>2</sub> were purchased from Sigma-Aldrich and used as received.

Voltammetric experiments were performed with a Biologic VMP3/Z multi-channel potentiostat using a standard 3-electrode set-up, with a Pt wire counter electrode. A Ag/Ag<sup>+</sup> reference electrode was made by immersing a silver wire into a 5 mM AgCl [P<sub>6,6,6,14</sub>]Cl solution separated from the bulk solution with a porous frit. Glassy carbon (1 mm diameter, ALS Co., Ltd. Japan) was used as the working electrode for cyclic voltammetry experiments.

Prior to any scan, the working electrode was polished with alumina and then washed with deionised water (Millipore SuperQ system, resistivity 18.2 M $\Omega$  cm<sup>-1</sup>). The measurements were carried out with an IR drop compensation prior to the cyclic voltammetry

experiments compensating approximately 85% of the total internal resistance.

The ionic liquids were bubbled with oxygen (ultrahigh purity grade, Air Liquide) for 30 min prior to performing the voltammetry measurements, and bubbled again between scans. Control N<sub>2</sub>-saturated experiments were performed by bubbling the ionic liquid with nitrogen (ultrahigh purity grade, Air Liquide) for 30 min to remove the oxygen. All of the experiments were performed at 20 ± 1 °C and a scan rate of 10 mV s<sup>-1</sup>.

The diffusion coefficients and saturated concentrations of oxygen for the neat ionic liquids were determined by cyclic voltammetry using a carbon fiber ultramicroelectrode (7 micrometer diameter, ALS Co., Ltd. Japan) for steady state current and chronoamperometry experiments using a glassy carbon electrode (1 mm diameter, ALS Co., Ltd. Japan). The steady-state current,  $i_{ss}$ , with an ultramicroelectrode having radius  $r_0$  is given by the following equation:

$$i_{ss} = 4nFDc_0r_0 \quad (2)$$

The current density at a disk macro-electrode is proportional to the square root of time as represented by Cottrell's equation:

$$j(t) = \frac{nFD^{1/2}}{\pi^{1/2}t^{3/2}} \quad (3)$$

Therefore, the diffusion coefficient ( $D$ ) and solubility of oxygen ( $C$ ) were calculated from the terms  $DC$  and  $D^{1/2}C$  obtained from equations 2 and 3 at 20 ± 1 °C.

Conductivity measurements were performed via electrochemical impedance spectroscopy using a Biologic SP200 potentiostat, and viscosity measurements were performed with a SV-1A vibro viscometer. Differential scanning calorimetry (DSC) was performed with a Mettler Toledo DSCI STAR<sup>e</sup> system scanning between -125 °C and 0 °C at a scan rate of 40 ° min<sup>-1</sup> during the cooling scan and the temperature values were calibrated using cyclohexane. 40 μl aluminum crucibles were used.

To measure self-diffusion coefficients for IL cations and anions, the simple and robust pulsed-gradient stimulated-echo sequence (PGSTE)<sup>25</sup> was applied for all measurements at 20 °C (± 0.5). A Bruker Avance III WB 500 MHz (11.0 T) NMR was equipped with a Diff50 pulse-field-gradient diffusion probe using a maximum gradient value of 1700 G/cm along spectrometer field ( $z$ ) axis and a 5 mm <sup>1</sup>H/<sup>13</sup>C rf coil. The PGSTE sequence used a  $\pi/2$  pulse time of 6.9 μs, sinusoidal gradient pulse with a duration  $\delta$  of 3.14 ms, diffusion time  $\Delta$  of 20 ms, The number of scans for each gradient

step was adjusted from 1-64 to ensure sufficient signal-to-noise ratio. 16 gradient steps were applied for each diffusion experiment, and the maximum gradient strength was adjusted to achieve ≥ 90% NMR signal attenuation. The NMR signal attenuation due to diffusion follows the Stejskal-Tanner equation<sup>26</sup>

$$I = I_0 e^{-D\gamma^2 g^2 \delta^2 (\Delta - \frac{\delta}{3})} \quad (4)$$

where  $I$  and  $I_0$  refer to the spin-echo signal intensity and spin-echo signal intensity at zero gradient, respectively,  $\gamma$  is the gyromagnetic ratio of the nucleus,  $g$  is the gradient strength,  $\delta$  is the pulse duration time and  $\Delta$  is the diffusion time. Thus, diffusion coefficients ( $D$ ) of a desired nucleus can be obtained by fitting the experimental  $I$  vs  $g$  data using equation 4.

All <sup>31</sup>P NMR spectroscopy was performed at 20 ± 0.5 °C using a Bruker Avance III 11.0 T spectrometer equipped with a 5 mm axial saddle coil. <sup>31</sup>P NMR was carried out using a simple  $\pi/2$  pulse time of 7.0 μs, relaxation delay time of 1s, and 32 scans per spectrum.

Density functional theory calculations were carried out using Gaussian 09.<sup>27</sup> For all species full conformational searches were carried out to ensure that global minima were located and frequency calculations were performed to ensure that convergence to a local minimum was achieved. Complexes of the cations [N<sub>1,1,1,1</sub>]<sup>+</sup> and [P<sub>1,1,1,1</sub>]<sup>+</sup> with the oxygen species O<sub>2</sub>, the superoxide radical anion O<sub>2</sub><sup>•-</sup>, or the di-anion species O<sub>2</sub><sup>2-</sup> were optimized at the UM06-2X/aug-cc-pVDZ level<sup>28,29</sup> in an ethanol solvent field represented by the conductor-like polarizable continuum model (CPCM).<sup>30,31</sup> The complex of the larger cation [P<sub>2,2,2,2</sub>]<sup>+</sup> with superoxide was also optimized to examine the effect of steric hindrance around the phosphonium centre. The optimized complexes were examined for evidence of covalent bonding between the cation and the oxygen through the measurement of intermolecular distances and by examining molecular orbitals. Gaussian archive entries for systems in this study are presented in Table S1.

### 3. Results and discussion

#### Electrochemical measurements

Figure 1 depicts the cyclic voltammograms obtained with the N<sub>2</sub>-saturated and O<sub>2</sub>-saturated neat phosphonium-based ionic liquids. The N<sub>2</sub>-saturated ionic liquids presented only small currents between -2 and +1 V vs Ag/Ag<sup>+</sup>, therefore the potential was scanned until -2 V vs Ag/Ag<sup>+</sup> in the case of the O<sub>2</sub>-saturated ionic liquids.

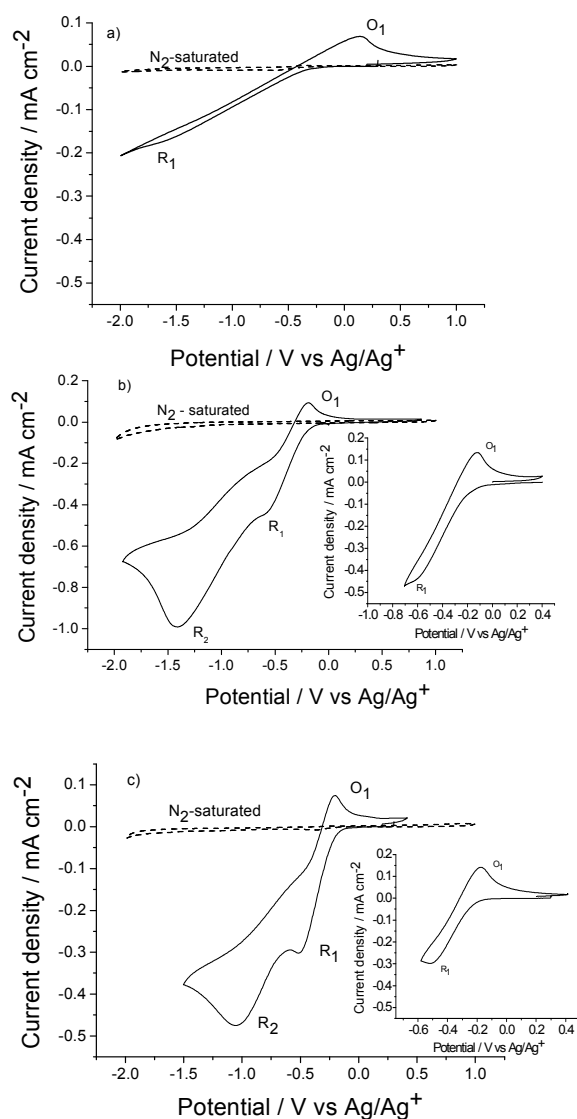


**Figure 1.** Cyclic voltammograms for the  $N_2$ -saturated, neat phosphonium-based ionic liquids and the reduction processes in the  $O_2$ -saturated neat phosphonium-based ionic liquids a)  $[P_{6,6,6,14}]Cl$ , b)  $[P_{6,6,6,14}][NTf_2]$ , and c)  $[P_{6,6,6,14}][dca]$ , with glassy carbon as the working electrode (1 mm diameter). Inset: cyclic voltammetry for the  $O_2$ -saturated ILs, scanning only until the first reduction process. Scan rate:  $10 \text{ mV s}^{-1}$

One chemically reversible reduction process,  $R_1$  and one irreversible reduction process  $R_2$ , were observed for the neat  $[P_{6,6,6,14}][NTf_2]$ , and  $[P_{6,6,6,14}][dca]$ , while only one chemically reversible reduction process was observed for the chloride ionic liquid analogue.

The first chemically reversible reduction process, ( $R_1/O_1$ ) attained for each of the phosphonium-based ILs in the series (Figure 1a, Figure 1b inset and Figure 1c inset) was assigned to the  $O_2/O_2^{\bullet-}$  redox couple, in good agreement with previous work on the oxygen reduction reaction in dry ionic liquids.<sup>11</sup>

The second reduction process ( $R_2$ ) is assigned to the reduction of the superoxide anion to the peroxide anion ( $O_2^{2-}$ ), as already established

in the literature describing oxygen reduction in a series of imidazolium and quaternary ammonium-based ILs.<sup>11,32,33</sup>

The increase in the number of electrons exchanged in the reduction of oxygen from one in neat  $[P_{6,6,6,14}]Cl$  to two in the case of neat  $[P_{6,6,6,14}][dca]$  and  $[P_{6,6,6,14}][NTf_2]$  holds importance for the use of air cathodes in electrochemical devices such as metal-air batteries. This difference in the number of electrons exchanged in the phosphonium-based ionic liquids series is attributed to the different mass transport properties, which will be explained in the following sections. It is also important to highlight at this point that our previous research work has been focused on the effect of weak protic additives in the ORR of  $[P_{6,6,6,14}]Cl$  which enhance the mass transport conditions in the ionic liquid. Subsequently, significant differences were observed in the number of electron exchanged upon addition of such additives, from one electron in the case of neat  $[P_{6,6,6,14}]Cl$  to two electrons in the case of  $[P_{6,6,6,14}]Cl$  mixtures.

The substantial peak potential separation observed for the reduction process ( $R_1/O_1$ ) in the case of  $[P_{6,6,6,14}]Cl$  ( $\Delta E_p \sim 2V$ ) suggests a slow mass transfer related to the unfavourable physical properties of the medium (conductivity =  $2.5 \times 10^{-6} \text{ S cm}^{-1}$  and viscosity  $> 1200 \text{ mPa s}$  at  $20^\circ\text{C}$ ), as opposed to the analogous  $[P_{6,6,6,14}][dca]$  and  $[P_{6,6,6,14}][NTf_2]$  (Figure 1 b and c) which presented superior conductivities ( $6.8 \times 10^{-5} \text{ S cm}^{-1}$  and  $6.1 \times 10^{-5} \text{ S cm}^{-1}$ , respectively at  $20^\circ\text{C}$ ) and viscosities (474 and 369 mPa s, respectively at  $20^\circ\text{C}$ ) (

Table 1). Therefore, the  $[dca]^-$  and  $[NTf_2]^-$  - based ionic liquids exhibited smaller peak potential separations,  $\Delta E_p = 0.32 \text{ V}$ , and  $0.50 \text{ V}$  respectively, in comparison to the chloride IL, due to these enhanced mass transport conditions.

Interestingly, despite the relatively similar conductivities and viscosities for the  $[dca]^-$  and  $[NTf_2]^-$  based ILs, the peak potential separation for the ( $R_1/O_1$ ) process was still slightly different. Therefore, other contributing factors such as their heterogeneous electron transfer kinetics and surface reactions must also have an impact on the peak to peak separation in these cases.<sup>34</sup>

**Table 1.** Conductivity, viscosity, glass transition temperature ( $T_g$ ), diffusion coefficient ( $D_{O_2}$ ) and solubility of oxygen ( $C_{O_2}$ ) in different phosphonium-based ionic liquids at  $20^\circ\text{C}$ .

Ionic liquid	$D_{anion} \times 10^{-8}$ ( $\text{cm}^2 \text{ s}^{-1}$ )	$D_{cation} \times 10^{-8}$ ( $\text{cm}^2 \text{ s}^{-1}$ )
$[P_{6,6,6,14}]Cl$	-	$0.28 \pm 0.08$
$[P_{6,6,6,14}][dca]$	$2.39 \pm 0.09$	$1.5 \pm 0.05$
$[P_{6,6,6,14}][NTf_2]$	$2.27 \pm 0.09$	$1.7 \pm 0.05$

When analysing Figure 1, a major difference in  $R_1$  peak current density is also observed in the case of  $[P_{6,6,6,14}][NTf_2]$   $-0.47 \text{ mA cm}^{-2}$  compared with  $-0.30 \text{ mA cm}^{-2}$  for the dca-based IL. It is likely that this is at least in part related to the reactant concentration in the medium, in this case oxygen. Table 1 lists the measured oxygen solubility ( $C$ ) for each of the ILs, with the value of dissolved oxygen in  $[P_{6,6,6,14}][NTf_2]$  being slightly greater in comparison with  $[P_{6,6,6,14}][dca]$  ( $9.8 \times 10^{-6}$  and  $9.1 \times 10^{-6} \text{ mol cm}^{-3}$ , respectively). This increase in oxygen solubility for the  $NTf_2$ -based ionic liquid could be due to the affinity between oxygen and fluorine as previously observed in highly fluorinated media.<sup>35</sup> The high viscosity of the neat  $[P_{6,6,6,14}][Cl]$  prevented the attainment of a steady-state currents in the measurement of  $D$  and  $C$  following equation 2 and 3. Nonetheless, the differences in diffusivity and oxygen solubility are not sufficient to explain the difference in peak currents; the clear diffusion-limit shape to the peaks suggests that perhaps the diffusion of the reduction products is limiting. The distinctly lower viscosity of the  $NTf_2$  IL suggests that the diffusivity of the products would be higher in that medium.

The solubility and diffusion coefficient of oxygen in  $[P_{6,6,6,14}][NTf_2]$  have been previously reported in the literature at  $35^\circ\text{C}$  by a number of authors. Evans *et al.*<sup>18</sup> obtained a concentration of  $6 \times 10^{-6} \text{ mol cm}^{-3}$  and diffusion coefficient of  $7.5 \times 10^{-6} \text{ cm}^2 \text{ s}^{-1}$ ; these are in accord with the  $C$  and  $D$  values determined in this work, taking into account the differences in temperature. However, Hayyan *et al.*<sup>19</sup> reported higher oxygen solubility for the same ionic liquid at  $35^\circ\text{C}$  ( $C = 11.9 \times 10^{-6} \text{ mol cm}^{-3}$ ) which was attributed to the acidic character of the ionic liquid. This may arise from residual acid impurities formed during the IL synthesis which can be common in these ILs, and thus can lead to instability of the superoxide<sup>19</sup>. It is important to note that these solubilities are considerably higher than that of oxygen in water and hence represent a potentially significant advantage over aqueous electrolytes for air-electrode devices.

#### Nuclear magnetic resonance (NMR) spectroscopy characterisation

In order to better understand oxygen transport in this series of phosphonium based ILs, we measured diffusion coefficients for each of the anions and cations using the pulse-field-gradient (PFG) NMR method (Table 2).<sup>25, 26</sup> PFG NMR allows for accurate and precise determination of  $D$  for separate molecular species. In this case, due to instrumental limitations we were able to measure  $D$  for all ions but  $Cl^-$ . We noticed that  $D$  for  $[NTf_2]^-$  and  $[dca]^-$  based ILs are quite similar, both for the anions and cations, as one would expect from their similar viscosities.

The anions diffuse  $\sim 50\%$  faster than the cations in these liquids, in contrast to many ILs,<sup>36, 37</sup> due to the large cation size relative to the anions. If one were to use only gas phase ion-size estimates in the Stokes-Einstein equation, one could expect the anions in these systems to diffuse a factor of 3-4 times faster than the cations, but ion aggregation effects reduce this difference.<sup>37, 38</sup> Furthermore, we see that  $D$  for the IL ions is a factor of 100 times slower than the oxygen diffusion measured electrochemically (Table 1); to an extent this is expected from the Stokes Einstein equation based on the size difference between the species (i.e. ionic radii for  $[P_{6,6,6,14}]^+$ :  $5.83 \text{ \AA}$ ,<sup>39</sup> and for  $O_2$ :  $1.3 \text{ \AA}$ ). However, the difference in ion size cannot explain all of this 100 fold higher diffusivity for oxygen.

The structure of the liquid may be complex at the nano-level; where aggregation of long alkyl chains due to a combination of electrostatics and the hydrophobic effects can result in the formation

of domains.<sup>40, 41</sup> Canongia Lopes and Padua,<sup>42</sup> noted by computer simulations the presence of hydrophilic domains that are formed by the head groups of the cations and anions and of nonpolar domains that are formed by the alkyl groups.<sup>41</sup> This has also been confirmed by Triolo *et al.*<sup>43</sup> using X-ray scattering experiments on 1-alkyl-3-methylimidazolium salts. In the present case the large alkyl chains of the phosphonium cation should certainly be expected to produce hydrophobic domains.

**Table 2.** Diffusion coefficient of anions ( $D_{anion}$ ) and cation ( $D_{cation}$ ) at  $20^\circ\text{C}$ .

Ionic liquid	Conductivity (S cm <sup>-1</sup> )	Viscosity (mPa.s)	T <sub>g</sub> (°C)	C <sub>O<sub>2</sub></sub> x 10 <sup>6</sup> (mol cm <sup>-3</sup> )	D <sub>O<sub>2</sub></sub> x 10 <sup>6</sup> (cm <sup>2</sup> s <sup>-1</sup> )
$[P_{6,6,6,14}][Cl]$	$2.5 \times 10^{-6}$	> 1200	-57.2	-	-
$[P_{6,6,6,14}][dca]$	$6.8 \times 10^{-5}$	474	-59.2	$9.1 \pm 0.9$	$2.1 \pm 0.2$
$[P_{6,6,6,14}][NTf_2]$	$6.1 \times 10^{-5}$	369	-58.5	$9.8 \pm 0.7$	$1.7 \pm 0.1$

Therefore, the hydrophobic/hydrophilic nature of these domains will determine the oxygen mobility in the ionic liquid. The oxygen solubility has been studied in a variety of solvents,<sup>44</sup> and, as an example, the solubility of oxygen ( $C$ ) in water ( $1.2 \text{ mM}$  in a  $0.1 \text{ M KOH}$  aqueous solution at  $25^\circ\text{C}$ )<sup>45</sup> is much lower than in phosphonium-based ionic liquids<sup>46</sup> (e.g.  $9.8 \text{ mM}$  in  $[P_{6,6,6,14}][NTf_2]$  at  $20^\circ\text{C}$ , as determined in this work). Also in hydrophobic media, for a given temperature, the oxygen solubility increases with the length of alkyl chain in saturated hydrocarbons media.<sup>44</sup> Therefore, due to the long alkyl chains of  $[P_{6,6,6,14}]^+$ , it is likely that interconnected alkyl apolar domains exist in which the oxygen is predominantly dissolved and is more diffusive. In other words, the relatively slow diffusion of the IL ions that is determined by the PFG NMR diffusion measurement does not necessarily reflect the local dynamics of the apolar regions within which the oxygen is able to diffuse. In a sense, the oxygen diffusion is facilitated by these local dynamics, and is decoupled from the bulk viscosity of the IL.

Further developments of ILs for metal-air batteries might involve design of IL systems conducive to fast oxygen diffusion and high oxygen solubility using this idea, in addition to incorporation of additional fluorinated groups due to their known favourable interactions with oxygen.<sup>47</sup>

#### Stability of the superoxide species

Another interesting feature observed in the cyclic voltammograms depicted in Figure 1 is the pronounced asymmetry in the heights of the forward and reverse peaks in the cyclic voltammograms measured under  $O_2$ -saturated conditions. Several examples showing similar trends have been reported in the literature in dry ionic liquids; this asymmetry has been attributed either to large differences in the diffusion coefficients of the oxygen and the electrogenerated

superoxide anion, which can differ by a factor of  $30^6$  or to the reactivity of the superoxide anion towards the IL cation as reported for the imidazolium cation<sup>12</sup> and also  $[P_{6,6,6,14}]^+$ .<sup>11, 18</sup> Therefore, we have performed NMR studies to attempt to assess the degree of degradation of these ILs in the presence of the superoxide or peroxide anions. We used saturated solutions of  $KO_2$  and  $Na_2O_2$  in  $[P_{6,6,6,14}][NTf_2]$ , which were allowed to stand at room temperature for more than 1 month. When observing the  $^{31}P$  nucleus, as well as  $^{13}C$  and the  $^1H$  nuclei in the cation, and the  $^{13}C$  and  $^{19}F$  nuclei in the anions, no chemically distinct degradation products were observed; the estimated limit of detection in these experiments is  $\sim 0.1$  mol %. Representative spectra of  $^{31}P$  and  $^1H$  (and further experimental details) are shown in supporting information. It therefore appears that these ILs do not significantly breakdown due to the presence of  $O_2^{\bullet-}$  and  $O_2^{2-}$  over extended periods.

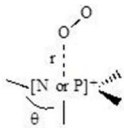
### Density functional theory calculations

To probe further the reasons for stabilisation of superoxide in phosphonium-based ILs, the interactions between charged oxygen species ( $O_2^{\bullet-}$ ,  $O_2^{2-}$ ) and the quaternary phosphonium cations were examined using computational quantum chemistry. Given the computational demands of such calculations, a smaller cation species was modelled,  $[P_{1,1,1,1}]^+$ . Comparisons with quaternary ammonium cations were performed, based on the reported high stability of electrogenerated superoxide ( $O_2^{\bullet-}$ ) in quaternary ammonium based ILs.<sup>11,18</sup> The stability in these cases is possibly due to the tendency to form a salt of tetramethylammonium superoxide  $[(CH_3)_4N][O_2]^{\bullet-}$ .

Optimized structures of the phosphonium and ammonium cations in association with the various oxygen species are shown in Table 3. The intermolecular approach distances between the nitrogen or phosphorus cation centres and the closest oxygen atoms are listed ( $r$ ) along with the  $C-[N \text{ or } P]-C$  bond angles ( $\theta$ ). These parameters give an indication of the level of interaction between the cation and the oxygen species. For complexes of  $[N_{1,1,1,1}]^+$  with  $O_2$ ,  $O_2^{\bullet-}$ , or  $O_2^{2-}$  and for complexes of  $[P_{1,1,1,1}]^+$  with  $O_2$ , the intermolecular distances are greater than 3 Å, and the  $C-[N \text{ or } P]-C$  bond angles are close to the tetrahedral bond angle of  $109.5^\circ$ . It is therefore clear that, for these species, the interaction between the molecules is entirely non-covalent in nature.

However, the  $[P_{1,1,1,1}]^+ - O_2^{\bullet-}$  complex shows a different geometry when optimization is performed in the presence of a solvent field than it does when the optimisation is performed in the gas phase (Table 3). Interestingly, in the gas phase, the intermolecular distance for the  $[P_{1,1,1,1}]^+ - O_2^{\bullet-}$  complex drops to 2.067 Å and the bond angle to  $95.9^\circ$ , indicating an increased interaction. However, in the solvent field the intermolecular distance is 3.128 Å and the bond angle is  $106.8^\circ$ . As discussed above, this is indicative of a non-covalent interaction between the cation and the superoxide, but this intermolecular distance is shorter and bond angle is greater than in the case of  $[N_{1,1,1,1}]^+ - O_2^{\bullet-}$  (i.e. 3.434 Å and  $109.8^\circ$ ), demonstrating that the quaternary phosphonium ion allows a slightly stronger interaction and thus can more effectively stabilise the  $O_2^{\bullet-}$  species.

**Table 3.** Intermolecular distances ( $r$ ), bond angles ( $\theta$ ) and optimized structures of complexes formed between phosphonium and ammonium cations and various oxygen species. Optimizations were performed at the UM06-2X/aug-cc-pVDZ level in an ethanol solvent field implemented using CPCM (unless otherwise stated). Atoms labels: blue=nitrogen, orange=phosphorus, red=oxygen, grey=carbon, white=hydrogen.



Cation	Dioxygen	$r/\text{\AA}$	$\theta/^\circ$	Optimized structure
$[N_{1,1,1,1}]^+$	$O_2$	3.836	109.5	
	$O_2^{\bullet-}$	3.434	109.8	
	$O_2^{2-}$	3.221	110.4	
$[P_{1,1,1,1}]^+$	$O_2$	3.679	109.1	
	$O_2^{\bullet-}$	3.128	106.8	
	$O_2^{\bullet-}$ (gas phase)	2.067	95.9	
	$O_2^{2-}$	1.787	89.5	
$[P_{2,2,2,2}]^+$	$O_2^{\bullet-}$	2.892	105.7	

When the  $[P_{1,1,1,1}]^+$  cation is complexed with the di-anionic species,  $O_2^{2-}$ , a short intermolecular distance is seen in the solvated optimized structures. In ethanol the  $P-O$  distance is only 1.787 Å. For comparison,  $P-O(H)$  distances of 1.568-1.577 Å are observed in

crystalline phosphoric acids,<sup>49</sup> and 1.60 Å in 3.84 mol% aqueous H<sub>3</sub>PO<sub>4</sub>.<sup>50</sup> The [P<sub>1,1,1,1</sub>]<sup>+</sup>—O<sub>2</sub><sup>2-</sup> complex adopts a trigonal bipyramidal geometry with C—P—C bond angles of close to 90.0° between the axial and equatorial methyl groups and 120.1° between the equatorial methyl groups. Thus this calculation clearly indicates that a covalent bonding interaction can occur in this complex. When we examine the molecular orbitals, the second highest molecular orbital (HOMO-1) clearly shows the bonding interaction between the cation and O<sub>2</sub><sup>2-</sup> (see Figure 2). Similar bonding is seen in the HOMO of the gas phase [P<sub>1,1,1,1</sub>]<sup>+</sup>—O<sub>2</sub><sup>•-</sup> species, but the bonding is no longer present for the same structure optimized in a solvent field as observed in Table 3. However, the P—O distance in the latter case is still shorter than is observed for the ammonium analogue and short enough to be a significant interaction.

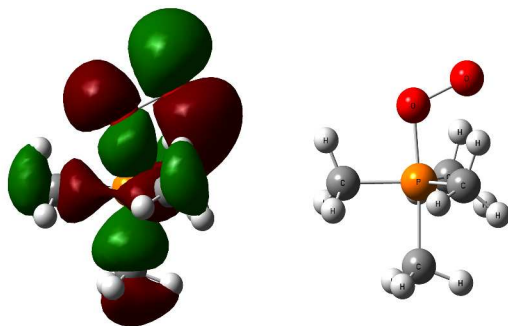


**Figure 2.** Bonding orbital (HOMO-1) of the [P<sub>1,1,1,1</sub>]<sup>+</sup>—O<sub>2</sub><sup>2-</sup> species at the UM06-2X/aug-cc-pVDZ level in an ethanol solvent field. For clarity the same molecular orientation is also shown with the orbital lobes removed.

The complex of the larger cation [P<sub>2,2,2,2</sub>]<sup>+</sup> with superoxide was also optimized to examine the effect of steric hindrance around the phosphonium centre. The [P<sub>2,2,2,2</sub>]<sup>+</sup>—O<sub>2</sub><sup>•-</sup> structure optimized in solvent shows a similar non-covalent interaction to that seen in [P<sub>1,1,1,1</sub>]<sup>+</sup>—O<sub>2</sub><sup>•-</sup>. The slightly shorter P—O intermolecular distance of 2.892 Å indicates that the planar arrangement of the three ethyl substituents presents no additional steric hindrance around the phosphonium centre. The C—P—C bond angle of  $\theta = 105.7^\circ$  is close to the angle of 106.8° seen for the tetramethyl cation, and is indicative of a non-covalent interaction between the cation and the superoxide.

Thus it appears that there is a close, but non-covalent, interaction between the superoxide ion and the phosphorous atom in the phosphonium cations that is not present between superoxide and nitrogen in the analogous ammonium cations and this close interaction stabilises the superoxide. Given the trend observed from [P<sub>1,1,1,1</sub>]<sup>+</sup> to [P<sub>2,2,2,2</sub>]<sup>+</sup> it seems probable that a similar interaction will remain when larger alkyl chains are present, such as in [P<sub>6,6,6,14</sub>]<sup>+</sup>, however this remains to be confirmed when the larger calculations required can be carried out.

### Protic Additives

Finally, the role of acidic moieties in the stability of the O<sub>2</sub>/O<sub>2</sub><sup>•-</sup> redox couple in [P<sub>6,6,6,14</sub>]Cl has been studied here via addition of hydrochloric acid, (a common side product in phosphonium-based

ILs synthesis)<sup>51</sup> by cyclic voltammetry. Figure 3 gives an example of the detrimental effect of HCl on the reversibility of the O<sub>2</sub> redox process. In the presence of HCl the reduction process for oxygen is irreversible<sup>21</sup> as opposed to the pure [P<sub>6,6,6,14</sub>]Cl where chemical reversibility of the electrogenerated superoxide anion is observed.

Thus, it seems plausible that the instability of the superoxide anion O<sub>2</sub><sup>•-</sup> in [P<sub>6,6,6,14</sub>]<sup>+</sup> that has previously been observed by other workers<sup>18</sup> could be related to the presence of residual acidic impurities. As a corroborating example, improvement in the stability of the superoxide anion has been observed in tetraglyme, when comparing as-received and distilled tetraglyme, because of reaction between the superoxide and impurities in the as-received sample.<sup>52</sup> Therefore, we conclude that the purity of the ionic liquids is crucial for attaining the reversible O<sub>2</sub>/O<sub>2</sub><sup>•-</sup> redox couple.

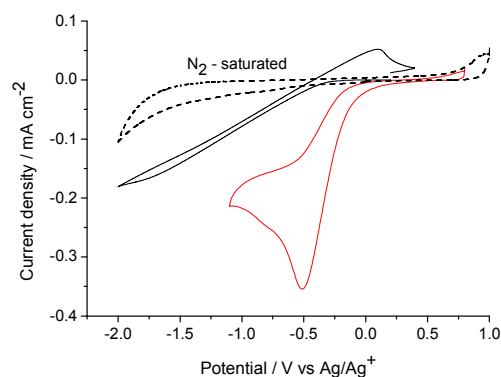


**Figure 3.** Cyclic voltammograms of the O<sub>2</sub>-saturated [P<sub>6,6,6,14</sub>]Cl in the absence (—) and in the presence of 1.8 wt% HCl (—). N<sub>2</sub>-saturated [P<sub>6,6,6,14</sub>]Cl in the presence of 1.8 wt% HCl (dashed line).

### 4. Conclusions

In this work we have used computational quantum chemistry to examine more closely the interactions between differently charged oxygen species and quaternary phosphonium and ammonium cations. A shorter intermolecular distance between the quaternary phosphonium cation and the superoxide and higher bond angles were observed, in comparison with those of the quaternary ammonium, which is known for its ability to stabilise the superoxide anion.

By determining the physical properties of the neat ionic liquids (including conductivity, viscosity, and individual ion diffusion coefficients, oxygen diffusion coefficient and oxygen solubility) it was shown that these factors play an important role in the oxygen reduction reaction in terms of number of electrons exchanged, mass transport kinetics and current density.

In cyclic voltammetry, the dca-based ionic liquid exhibited the lowest peak potential separation in the series (dca  $\Delta E_p = 0.32$  V < NTf<sub>2</sub>  $\Delta E_p = 0.5$  V < Cl<sup>-</sup>  $\Delta E_p = 2$  V). This discrepancy was partially attributed to mass transport, but heterogeneous electron transfer kinetics and surface reactions could be a factor affecting the peak to peak separation that will require further investigation.

The peak current density for the reduction process  $O_2/O_2^{\bullet-}$  is superior for  $[P_{6,6,6,14}][NTf_2]$  in comparison with that of  $[P_{6,6,6,14}][dca]$  because of the higher oxygen concentration in the media resulting from the affinity between the fluorine-bearing anions and oxygen.

NMR diffusion measurements indicate that oxygen diffusion is essentially decoupled from IL diffusion for these systems. The formation of an interconnected hydrophobic phase composed of the apolar long alkyl chains of  $[P_{6,6,6,14}]^+$ , as observed in numerous IL systems would serve to promote fast oxygen diffusion without the need for IL ion translation. Thus this study helps to point the way towards rational design of new ILs to support high solubility and fast diffusion of oxygen for use in electrochemical devices.

## Acknowledgements

The authors gratefully acknowledge financial support from the Australian Research Council (ARC) through the ARC Centre of Excellence for Electromaterials Science (ACES). MF and DRM are grateful to the Australian Research Council for support under the Australian Laureate Fellowship scheme. LAM was supported in part by the National Science Foundation (USA) under award number DMR-0844933.

We gratefully acknowledge generous allocations of computing time from the National Facility of the National Computational Infrastructure (Canberra, Australia) and the Monash Campus Cluster at the eResearch Centre of Monash University, Australia. The authors also thank Cytec for the provision of the phosphonium-based ionic liquid  $[P_{6,6,6,14}][dca]$ .

## Notes and references

<sup>a</sup>ARC Centre of Excellence for Electromaterials Science, IFM-Institute for Frontier Materials, Deakin University, 221 Burwood Hwy, Burwood, Victoria 3125, Australia.

<sup>b</sup>ARC Centre of Excellence for Electromaterials Science, Monash University, Clayton, Victoria 3800, Australia.

<sup>c</sup>Department of Chemistry and Macromolecules and Interfaces Institute, Virginia Tech, Blacksburg, VA 24061 USA

† Electronic Supplementary Information (ESI) available: <sup>31</sup>P and <sup>1</sup>H NMR on  $[P_{6,6,6,14}][NTf_2]$  and its solutions with  $KO_2$  and  $Na_2O_2$  and Gaussian archive entries for systems in this study.

- J.-S. Lee, S. Tai Kim, R. Cao, N.-S. Choi, M. Liu, K. T. Lee and J. Cho, *Advanced Energy Materials*, 2011, **1**, 34-50.
- M. Balaish, A. Kraytsberg and Y. Ein-Eli, *Phys Chem Chem Phys*, 2014, **16**, 2801-2822.
- J. B. Goodenough and K.-S. Park, *J Am Chem Soc*, 2013, **135**, 1167-1176.
- C. J. Allen, J. Hwang, R. Kautz, S. Mukerjee, E. J. Plichta, M. A. Hendrickson and K. M. Abraham, *J. Phys. Chem. C*, 2012, **116**, 20755-20764.
- K. M. Abraham, *ECS Transactions*, 2008, **3**, 67-71.
- M. C. Buzzeo, O. V. Klymenko, J. D. Wadhawan, C. Hardacre, K. R. Seddon and R. G. Compton, *The Journal of Physical Chemistry A*, 2003, **107**, 8872-8878.
- Y. Che, M. Tsushima, F. Matsumoto, T. Okajima, K. Tokuda and T. Ohsaka, *The Journal of Physical Chemistry*, 1996, **100**, 20134-20137.
- M. Balaish, A. Kraytsberg and Y. Ein-Eli, *Physical Chemistry Chemical Physics*, 2014.
- D. Zhang, T. Okajima, F. Matsumoto and T. Ohsaka, *Journal of the Electrochemical Society*, 2004, **151**, D31-D37.
- D. R. MacFarlane, N. Tachikawa, M. Forsyth, J. M. Pringle, P. C. Howlett, G. D. Elliott, J. H. Davis, M. Watanabe, P. Simon and C. A. Angell, *Energy & Environmental Science*, 2014, **7**, 232-250.
- Y. Katayama, H. Onodera, M. Yamagata and T. Miura, *Journal of the Electrochemical Society*, 2004, **151**, A59-A63.
- X. Z. Yuan, V. Alzate, Z. Xie, D. G. Ivey, E. Dy and W. Qu, *Journal of the Electrochemical Society*, 2014, **161**, A458-A466.
- E. E. Switzer, R. Zeller, Q. Chen, K. Sieradzki, D. A. Buttry and C. Friesen, *Journal of Physical Chemistry C*, 2013, **117**, 8683-8690.
- X.-Z. Yuan, V. Alzate, Z. Xie, D. G. Ivey and W. Qu, *Journal of the Electrochemical Society*, 2014, **161**, A451-A457.
- M. T. Carter and C. L. Hussey, *Inorganic Chemistry*, 1991, **30**, 1149-1151.
- I. M. AlNashef, M. L. Leonard, M. C. Kittle, M. A. Matthews and J. W. Weidner, *Electrochem. Solid State Lett.*, 2001, **4**, D16-D18.
- M. Hayyan, F. S. Mjalli, I. M. AlNashef and M. A. Hashim, *Journal of Fluorine Chemistry*, 2012, **142**, 83-89.
- R. G. Evans, O. V. Klymenko, S. A. Saddoughi, C. Hardacre and R. G. Compton, *Journal of Physical Chemistry B*, 2004, **108**, 7878-7886.
- M. a. Hayyan, M. A. Hashim, I. M. a. AlNashef, X. M. b. Tan and K. L. Chooi, *Journal of Applied Science*, 2010, **10**, 1176-1180.
- C. Pozo-Gonzalo, A. A. J. Torriero, M. Forsyth, D. R. MacFarlane and P. C. Howlett, *J. Phys. Chem. Lett.*, 2013, **4**, 1834-1837.
- C. Pozo-Gonzalo, C. Virgilio, Y. Yan, P. C. Howlett, N. Byrne, D. R. MacFarlane and M. Forsyth, *Electrochemistry Communications*, 2014, **38**, 24-27.
- T. Khoo, P. C. Howlett, M. Tsagouria, D. R. MacFarlane and M. Forsyth, *Electrochimica Acta*, 2011, **58**, 583-588.
- M. Kar, B. Winther-Jensen, M. Forsyth and D. R. MacFarlane, *Phys Chem Chem Phys*, 2014, **16**, 10816-10822.
- Y. Yan, T. Khoo, C. Pozo-Gonzalo, A. F. Hollenkamp, P. C. Howlett, D. R. MacFarlane and M. Forsyth, *J. Electrochem. Soc.*, 2014, **161**, A974-A980.
- J. E. Tanner, *Journal of Chemical Physics*, 1970, **52**, 2523-2526.
- E. O. Stejskal and J. E. Tanner, *Journal of Chemical Physics*, 1965, **42**, 288-292.
- M. J. T. Frisch, G. W.; Schlegel, H. B.; Scuseria, G. E.; Robb, M. A.; Cheeseman, J. R.; Montgomery, J. A.; Jr., T. V.; Kudin, K. N.; Burant, J. C.; Millam, J. M.; Iyengar, S. S.; Tomasi, J.; Barone, V.; Mennucci, B.; Cossi, M.; Scalmani, G.; Rega, N.; Petersson, G. A.; Nakatsuji, H.; Hada, M.; Ehara, M.; Toyota, K.; Fukuda, R.; Hasegawa, J.; Ishida, M.; Nakajima, T.; Honda, Y.; Kitao, O.; Nakai, H.; Klene, M.; Li, X.; Knox, J.

- E.; Hratchian, H. P.; Cross, J. B.; Bakken, V.; Adamo, C.; Jaramillo, J.; Gomperts, R.; Stratmann, R. E.; Yazyev, O.; Austin, A. J.; Cammi, R.; Pomelli, C.; Ochterski, J. W.; Ayala, P. Y.; Morokuma, K.; Voth, G. A.; Salvador, P.; Dannenberg, J. J.; Zakrzewski, V. G.; Dapprich, S.; Daniels, A. D.; Strain, M. C.; Farkas, O.; Malick, D. K.; Rabuck, A. D.; Raghavachari, K.; Foresman, J. B.; Ortiz, J. V.; Cui, Q.; Baboul, A. G.; Clifford, S.; Cioslowski, J.; Stefanov, B. B.; G. Liu, A. L.; Piskorz, P.; Komaromi, I.; Martin, R. L.; Fox, D. J.; Keith, T.; Al-Laham, M. A.; Peng, C. Y.; Nanayakkara, A.; Challacombe, M.; Gill, P. M. W.; Johnson, B.; Chen, W.; Wong, M. W.; Gonzalez, C.; Pople, J. A., , *GAUSSIAN 09*, (2009) Revision A.02. Gaussian, Inc., Wallingford CT.
28. Y. Zhao and D. Truhlar, *Theor Chem Account*, 2008, **120**, 215-241.
29. T. H. Dunning, *The Journal of Chemical Physics*, 1989, **90**, 1007-1023.
30. M. Cossi, N. Rega, G. Scalmani and V. Barone, *Journal of Computational Chemistry*, 2003, **24**, 669-681.
31. V. Barone and M. Cossi, *The Journal of Physical Chemistry A*, 1998, **102**, 1995-2001.
32. M. M. Islam and T. Ohsaka, *Journal of Physical Chemistry C*, 2008, **112**, 1269-1275.
33. A. Rene, D. Hauchard, C. Lagrost and P. Hapiot, *Journal of Physical Chemistry B*, 2009, **113**, 2826-2831.
34. D. T. Sawyer, A. Sobkowiak and J. L. Roberts, *Electrochemistry for chemists*, John Wiley & Sons, Inc., New York, 1995.
35. M. F. Costa Gomes, J. Deschamps and D. H. Menz, *Journal of Fluorine Chemistry*, 2004, **125**, 1325-1329.
36. H. Tokuda, K. Hayamizu, K. Ishii, M. Susan and M. Watanabe, *Journal of Physical Chemistry B*, 2005, **109**, 6103-6110.
37. J. B. Hou, Z. Zhang and L. A. Madsen, *Journal of Physical Chemistry B*, 2011, **115**, 4576-4582.
38. T. J. Simons, Z. Zhang, P. M. Bayley, P. C. Howlett, D. R. MacFarlane, L. A. Madsen and M. Forsyth, *Journal of Physical Chemistry B*, 2014, **118**, 4895-4905.
39. D. R. MacFarlane, M. Forsyth, E. I. Izgorodina, A. P. Abbott, G. Annat and K. Fraser, *Phys Chem Chem Phys*, 2009, **11**, 4962-4967.
40. K. Fruchey, C. M. Lawler and M. D. Fayer, *The Journal of Physical Chemistry B*, 2012, **116**, 3054-3064.
41. H. Weingärtner, *Angewandte Chemie International Edition*, 2008, **47**, 654-670.
42. J. N. A. Canongia Lopes and A. A. H. Pádua, *The Journal of Physical Chemistry B*, 2006, **110**, 3330-3335.
43. A. Triolo, O. Russina, H.-J. Bleif and E. Di Cola, *The Journal of Physical Chemistry B*, 2007, **111**, 4641-4644.
44. R. Battino, T. R. Rettich and T. Tominaga, *Journal of Physical and Chemical Reference Data*, 1983, **12**, 163-178.
45. R. Kerr, C. Pozo-Gonzalo, M. Forsyth and B. Winther-Jensen, *ECS Electrochemistry Letters*, 2013, **2**, F29-F31.
46. Y. Katayama, K. Sekiguchi, M. Yamagata and T. Miura, *Journal of the Electrochemical Society*, 2005, **152**, E247-E250.
47. L. C. Clark and F. Gollan, *Science*, 1966, **152**, 1755-1756.
48. D. T. Sawyer and J. S. Valentine, *Accounts of Chemical Research*, 1981, **14**, 393-400.
49. S. Furberg, *Acta Chemica Scandinavica* 1955, **89**, 1457-1460.
50. R. Caminiti, P. Cucca and D. Atzei, *The Journal of Physical Chemistry*, 1985, **89**, 1457-1460.
51. T. Khoo, A. Somers, A. A. J. Torriero, D. R. MacFarlane, P. C. Howlett and M. Forsyth, *Electrochimica Acta*, 2013, **87**, 701-708.
52. K. U. Schwenke, S. Meini, X. Wu, H. A. Gasteiger and M. Piana, *Phys Chem Chem Phys*, 2013, **15**, 11830-11839.